

ARCHIVES
of
FOUNDRY ENGINEERINGISSN (2299-2944)
Volume 2022
Issue 3/2022

5 – 10



10.24425/afe.2022.140230

1/3

Published quarterly as the organ of the Foundry Commission of the Polish Academy of Sciences

Corrosion Resistance of Cast Duplex Steels

P. Müller * , V. Pernica , V. Kaňa 

Brno University of Technology, Czech Republic

* Corresponding author. E-mail address: 183506@vutbr.cz

Received 07.12.2021; accepted in revised form 06.04.2022; available online 10.07.2022

Abstract

The aim of this work is to investigate the resistance of cast duplex (austenitic-ferritic) steels to pitting corrosion with respect to the value of PREN (Pitting Resistance Equivalent Number). Pitting corrosion is one of the most common types of corrosion of stainless steels. In most cases, it is caused by the penetration of aggressive anions through the protective passive layer of the steel, and after its disruption, it leads to subsurface propagation of corrosion. The motivation for the research was a severe pitting corrosion attack on the blades of the gypsum-calcium water mixer in a thermal power plant operation.

In order to examine the corrosion resistance, 4 samples of 1.4517 steel with different concentrations of alloying elements (within the interval indicated by the steel grade) and thus with a different PREN value were cast. The corrosion resistance of the samples was evaluated by the ASTM G48 – 11 corrosion test in a 6% aqueous FeCl₃ solution at room and elevated solution temperatures. To verify the possible effect of different alloying element concentrations on the mechanical properties, the research was supplemented by tensile and Charpy impact tests. Based on the results, it was found that a significant factor in the resistance of duplex steels to pitting corrosion is the temperature of the solution. For the components in operation, it is therefore necessary to take this effect into account and thoroughly control and manage the temperature of the environment in which the components operate.

Keywords: Cast duplex steel, Pitting resistance equivalent number, Ferric chloride, Critical pitting temperature, Mechanical properties

1. Introduction

1.1. Duplex stainless steels

The term duplex steel is usually understood as austenitic-ferritic steels. This convention will be used in the whole article. Thus, at room temperature, duplex steels consist of two phases – austenite and ferrite. Their proportion can vary, but usually, it is approximately the same (50-50%). Duplex steels thus combine the most important properties of ferritic (resistance to stress-corrosion cracking and pitting corrosion) and austenitic (high toughness) stainless steels. The corrosion resistance of duplex steels is similar to that of austenitic steels, although they are significantly more resistant to stress corrosion cracking and pitting corrosion. Duplex steels achieve higher strength than ferritic and austenitic stainless

steels, and ductility reaches values between ferritic and austenitic [1], [2], [3].

The limiting factor for duplex steels is the temperature range. Duplex steels have insufficient toughness at cryogenic temperatures (due to the brittle-ductile transition of ferrite) and at temperatures above 300 °C (which leads to precipitation of brittle phases), therefore, the best performance is achieved in – 100 to 300 °C, although it may vary between individual steel grades [4], [2].

1.2. Pitting corrosion

Pitting corrosion is one of the types of localized corrosion and belongs to electrochemical corrosion – it is accompanied by an anodic and cathodic reaction and is formed in the presence of an electrolyte.



The mechanism of pitting corrosion presupposes the formation of a stable pit, by fluctuating the passivation and depassivation events on the surface of the material. Once a stable pit is formed, its interior behaves as a sacrificial anode (i.e., the anode dissolves due to the corrosion process) and the surrounding metal as a cathode, where the oxidizing component (usually oxygen dissolved in the electrolyte) is reduced. The course of pitting corrosion is supported and accelerated by an increased concentration of activating ions, the presence of oxidizing substances (O_3 , ClO^-), but also increased temperature and low pH value [5].

Pitting corrosion is dangerous because its extent is often overlooked, the loss of material is extremely small, the pits are difficult to detect due to their size (in addition, they are covered with corrosion products). However, even with small visible damage, it can lead to mechanical failure of the part due to the holes it creates in the material. This can also lead to leakage of fluids through the material [6].

Passive layer breakdown and the formation of a pit

The formation of a stable pit is related to the properties of the passive layer and there are several mechanisms that describe it. The real phenomenon is often a combination of individual mechanisms. The **adsorption mechanism** describes the adsorption of aggressive anions from the solution (oxygen, hydroxide, or halide) at the surface of the passive layer, which leads to the migration of metal cations through the layer. If there is no migration of oxygen ions in the opposite direction, a cavity will form under the passive layer, which expands until part of the passive layer collapses because it has lost support. Another case is the **penetration mechanism**, in which the anions from the solution (mainly chloride) penetrate through the passive layer and behind this layer the anions react with the metal. The growth of the phase of the reaction products causes a local mechanical breakdown of the oxide passive layer. This mechanism is considered to be the main cause of pitting corrosion in an environment with chloride anions. The adsorption and penetration mechanism is shown in Fig. 1. At the same time, the material undergoes repassivation (i.e. the formation and renewal of the layer) and the transfer of electrons through the layer. These electrically compensate for the transfer of ions (depending on whether adsorption, penetration or repassivation occurs at a given location). The **film-breaking mechanism** appears under non-stationary conditions, i.e., changes in the potential in the layer. Sudden changes in the potential cause stress in the layer. This is due to chemical changes (e.g., a change in the valence of the element) and electrostriction (i.e., deformation of a non-conductor due to an external electric field). These stresses can cause a crack in the passive layer. In the presence of aggressive anions in the solution, they come into direct contact with the unprotected metal, which prevents repassivation at the crack site and leads to the formation of a pit [7].

Corrosion growth in a pit

Metal cations from the anodic reaction diffuse to the mouth of the pit, where they react with the hydroxide anion OH^- , which is formed during the cathodic reaction, and diffuse to the mouth of the pit by the electrolyte. The reaction results in metal hydroxide deposits which partially cover the surface of the pit. These corrosion products accelerate corrosion because they prevent the internal electrolyte inside the pit from mixing with the surrounding

electrolyte, resulting in a very acidic and aggressive environment inside the pit. Pitting corrosion often occurs on a horizontal surface, with gravity accelerating the growth of the pits downwards because at the tip of the pit the solution is significantly denser and more concentrated [6].

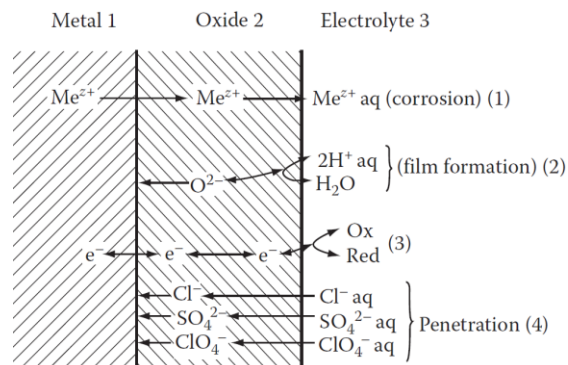


Fig. 1 Transfers of particles through the passive layer [7]

2. Experimental procedure

2.1. Description of the experiment

The aim of the experiment was to investigate the resistance of 1.4517 steel to pitting corrosion, depending on its chemical composition and the PREN (Pitting Resistance Equivalent Number) value. The standard test method ASTM G48 – 11 [8] was chosen to investigate the corrosion resistance. It describes the testing of stainless steels for the initiation of localized corrosion in a 6% aqueous solution of ferric chloride. The $FeCl_3$ solution is an extremely aggressive environment that causes corrosion in a shorter exposure time than in the common corrosive environments where parts work. The standard ASTM G48 – 11 specifies 6 test methods (A, B, C, D, E, F). Method A was chosen first - a pitting corrosion test at a constant room temperature, then at an elevated temperature of $55 \pm 7^\circ C$. Subsequently, method E was chosen (more in chapter 2.5).

The reason for the research was a corrosion attack on the blades of a gypsum-calcium water mixer in the operation of a thermal power plant. The corrosion attack led to mechanical damage and loss of the functionality of the blade.

2.2. Experiment design

Steel 1.4517 was examined. Steel grade 1.4517 specifies a wide range of elements content (Table 1). For this reason, different PREN values can be achieved with specific alloy contents (within the interval specified by the steel grade). The aim of the experiment was to investigate the corrosion resistance of steel 1.4517 at medium and elevated PREN values.

Table 1.

Chemical composition of steel grade 1.4517, mixer blade from operation and cast blocks.

| Material | %C | %Si | %Mn | %P | %S | %Cr | %Mo | %Ni | %N | %Cu | PREN ¹ | PREN ² |
|----------|-------|-------|-------|--------|-------|----------------|--------------|--------------|--------------|--------------|-------------------|-------------------|
| 1.4517 | 0.03 | 1.00 | 1.50 | 0.040 | 0.020 | 26.00 28.00 | 3.50 4.50 | 5.50 7.50 | 0.15 0.25 | 2.50 3.50 | 39.95 46.85 | 48.11 61.95 |
| Blade | 0.029 | 0.56 | 1.01 | 0.018 | 0.006 | 26.12 | 3.63 | 6.98 | 0.204 | 2.714 | 41.363 | 52.62 |
| Alloy 1 | 0.025 | 0.29 | 0.099 | 0.008 | 0.018 | 26.25 | 3.57 | 6.95 | 0.195 | 3.15 | 40.53 | 51.84 |
| Alloy 2 | 0.024 | 0.274 | 0.985 | 0.0089 | 0.018 | 26.21 | 3.546 | 6.906 | 0.201 | 2.973 | 41.13 | 52.12 |
| Alloy 3 | 0.024 | 0.283 | 0.847 | 0.0088 | 0.018 | 26.3 | 4.496 | 6.931 | 0.22 | 2.928 | 44.66 | 57.94 |
| Alloy 4 | 0.027 | 0.293 | 0.67 | 0.0094 | 0.019 | 26.83 | 4.454 | 6.8 | 0.312 | 2.879 | 46.52 | 65.28 |

¹ – PREN values calculated according to equation 1 [2]:

$$\text{PREN} = \% \text{Cr} + 3.3 \cdot (\% \text{Mo} + 0.5 \cdot \% \text{W}) + 16 \cdot \% \text{N} \quad (1)$$

² – PREN values calculated according to equation 2 [9]:

$$\text{PREN} = \% \text{Cr} + 3.3 \cdot \% \text{Mo} + 51 \cdot \% \text{N} + 6 \cdot \% \text{Mo} \cdot \% \text{N} - 1,6 \cdot \% \text{N}^2 \quad (2)$$

Steel 1.4517 was investigated at 4 different chemical compositions:

- Alloy 1 was designed to contain max. 0.15% of Mn. Since localized corrosion often initiates at MnS inclusions, to verify the effect of this phenomenon, the first alloy was selected with a reduced manganese content.
- Alloy 2 was designed to a chemical composition typical of steel grade 1.4517, i.e., to keep the content of the alloying elements in the middle of the specified interval.
- Alloy 3 was designed with the amount of molybdenum at the upper limit of the specified interval, in order to increase the PREN value.
- Alloy 4 was based on the composition of the third and, in contrast to it, designed with an increased nitrogen content and a slightly increased chromium content.

A test Y block (with a casting width of 60 mm) weighing about 20 kg was cast from each alloy. All the blocks were cast within one melt. After casting one alloy, the remaining melt was alloyed in the furnace to the desired composition of the next alloy. The melting took place in a vacuum induction furnace with the max. the capacity of 80 kg. Prior to casting Alloy 1, the furnace was evacuated in several phases, at a final pressure of 100 mbar for 20 minutes. The chemical composition of all the cast alloys is given in Table 1. The cast blocks were then subjected to solution annealing (5-hour stay at 1150 °C + 5-hour stay at 1040 °C, followed by cooling in water). Corrosion test specimens were then cut from the cast blocks. In addition to the cast specimens, the specimen cut from the stirrer blade, which failed in an operation, was also included in the corrosion test.

2.3. Preparation of the specimens

This subchapter describes the processes that all the specimens went through both for method A and method E. The specimens with the dimensions of 50x25x5 mm ± 1 mm were cut from the casting part of the block (the other part was the riser). The specimens were ground to a uniform surface quality, with the final grinding performed on the P120 grit sandpaper, on which the edges of the specimens were also rounded. The specimens were rinsed

thoroughly with water, cleaned with a cleaning paste, then rinsed in acetone and hot-air-dried. Until the test was performed, the specimens were stored in a desiccator. Before the test, their mass was measured to 0.0001 g.

All the corrosion tests were performed in 1000 ml glass beakers. The specimen in each of them was placed on a glass holder so that no surface of the specimen was in contact with the bottom / wall of the beaker. The position of the specimen in the beaker is shown in Fig. 2.



Fig. 2 Position of the specimen in a beaker

Subsequently, the specimens were immersed in a corrosive solution. The beakers were closed with plastic wrap and the specimens were left in the solution. The temperature of the solution and the immersion time of the specimen in it vary depending on the method. At the end of the specified time, the specimens were taken out and the corrosion products were brushed off. Then, the specimens were washed with water in an ultrasonic cleaner, rinsed with ethanol and hot-air-dried. Subsequently, their masses were measured, which were compared to the mass of the specimens before the test. The mass loss of each specimen was then expressed with respect to the size of its surface, making it possible to compare all the specimens, even if their dimensions differed by ± 1 mm.

2.4. Experiment method A

Solution: specimens were immersed in 600 ml of 6% aqueous solution of FeCl₃.

Test duration: 72 hours

Solution temperature: 1) room temperature (21.5 ± 2 °C);
2) 55 ± 7 °C

The experiment according to ASTM G48 – 11 method A was first performed at room temperature. In this experiment, all the specimens resisted the corrosive solution, the mass losses were zero. There were no visible signs of corrosion, neither in the visual inspection of the specimens nor in the metallographic observation of the microstructure. From this, it was possible to conclude that the observed steel is resistant to 6% FeCl₃ solution at room temperature, for all the investigated contents of the alloying elements.

Due to this result, the experiment was repeated (with new specimens) at elevated temperatures. To maintain a constant temperature, the beakers with the solution and the specimens were placed in water, in which an approximately constant temperature was maintained using an electric resistance heater (Fig. 3). The water temperature measurements revealed the water temperature as 55 ± 7 °C. The resulting mass losses and mass losses per area (i.e., outer surface of the specimens - area exposed to the solution) are given in Table 2.



Fig. 3 Test apparatus in temperature 55 ± 7 °C

Table 2.

Mass loss of the specimens at elevated (55 ± 7 °C) temperature

| | Blade | Alloy 1 | Alloy 2 | Alloy 3 | Alloy 4 |
|-----------------------------------|---------------|---------------|---------------|---------------|---------------|
| m_{bef} [g] | 52.1516 | 58.2678 | 54.4808 | 53.1401 | 55.3642 |
| m_{after} [g] | 47.5279 | 52.9381 | 49.4512 | 47.9027 | 53.598 |
| Δm [g] | 4.6237 | 5.3297 | 5.0296 | 5.2374 | 1.7662 |
| % m_{loss} | 8.87% | 9.15% | 9.23% | 9.86% | 3.19% |
| P [cm ²] | 33.0328 | 34.3394 | 33.1838 | 32.584 | 34.0702 |
| $\Delta m/P$ [g/cm ²] | 0.1400 | 0.1552 | 0.1516 | 0.1607 | 0.0518 |

m_{bef} – mass of the specimen before testing

m_{after} – mass of the specimen after testing

Δm – mass loss ($\Delta m = m_{\text{bef}} - m_{\text{after}}$)

% m_{loss} – relative mass loss (% $m_{\text{loss}} = \Delta m / m_{\text{bef}}$)

P – surface of the specimen

$\Delta m/P$ – mass loss per unit of surface area

Indications of corrosion, which appeared on the surface of each specimen, can be divided into 3 groups - colour indications, local surface protrusions and pits.

The specimens were then cross-sectioned, and metallographic specimens were made from the cross-sectional area for examination to further investigate the mechanisms of corrosion (Fig. 4, 5). The site of the cut was chosen at the site of a large indication of corrosion visible by visual inspection. The metallographic specimens were prepared by standard preparation procedures, i.e. they were successively ground and polished. Etching was performed with a Beraha II etchant to distinguish ferrite and austenite in the microstructure. The number of pits caused by corrosion on the main surface of the specimen (50x25 mm) was counted on the cross-section. Each pit of size >0.05 mm was considered a corrosion pit. The number of pits on the main surfaces of the samples is indicated in Table 3.

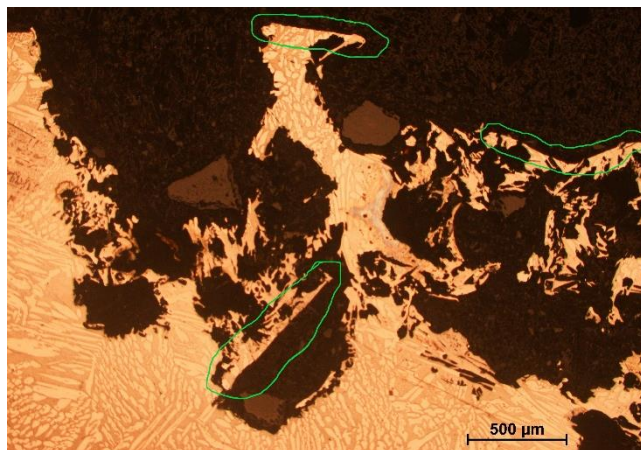


Fig. 4 Cross-section of a pit and the surrounding microstructure. Green ovals indicate the original surface of the specimen fallen inside the pit. Brown particles are mostly impurities from grinding and polishing

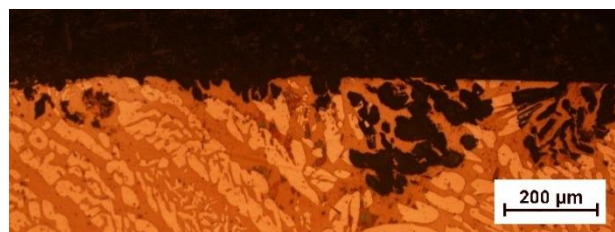


Fig. 5 Selective leaching of austenite grains in a pit

Table 3.

The number of pits caused by corrosion on the main surfaces of the specimens – evaluated on the cross section

| | Blade | Alloy 1 | Alloy 2 | Alloy 3 | Alloy 4 |
|----------------|-------|---------|---------|---------|---------|
| Number of pits | 11 | 30 | 26 | 23 | 1 |

Method E of the same standard for the corrosion resistance test (ASTM G48 - 11) was chosen due to the high fluctuation of the test temperature (55 ± 7 °C) and in order to investigate more thoroughly and accurately the corrosion resistance of each alloy at the elevated temperatures.

2.5. Experiment method E

Solution: the specimens were immersed in the solution, which consisted of 600 ml of water in which 6% FeCl₃ and 1% HCl had been dissolved

Test duration: 24 hours

Solution temperature: 1) 61 ± 1 °C; 2) 55 ± 1 °C;

The ASTM G48 - 11 method E consists in determining the CPT – critical pitting temperature – the lowest temperature at which pitting corrosion occurs. This procedure was chosen to better characterize the problem and compare the differences in the corrosion resistance of the investigated alloys. The theoretical estimate of CPT is described in equation 3. Based on this, the test temperature is selected (as the nearest increment rounded to 5 °C).

$$CPT = 2,5 \cdot \%Cr + 7,6 \cdot \%Mo + 31,9 \cdot \%N - 41,0 \quad (3)$$

If the specimen is attacked (meaning if pits with a size ≥ 0.025 mm form or when the value of the mass loss per area reaches ≥ 0.0001 g/cm²) at the selected test temperature, the next procedure is to perform the test again (with a new specimen and fresh solution) at a temperature 5 °C lower and repeat until the specimen passes the pitting corrosion test. Thus, the lowest temperature at which pitting corrosion occurred is the real CPT of the material.

Table 4.

Theoretical estimates of CPT for the examined alloys

| | Blade | Alloy 1 | Alloy 2 | Alloy 3 | Alloy 4 |
|--------------------|-------|---------|---------|---------|---------|
| estimated CPT [°C] | 58.4 | 58.0 | 57.9 | 65.9 | 69.9 |

Two sets of specimens were prepared for CPT detection. The temperature of the initial test was chosen to be 60 °C for all the specimens, according to Alloy 2, which has the lowest value of the theoretical estimate (eq. 3). Theoretical estimates of CPT for the alloys are given in Table 4.

The test was performed according to the defined procedure (although the temperature rose 1 °C higher) and the mass loss of each alloy was evaluated. Due to the test result at 60 °C, after which all the specimens were affected by corrosion, the temperature of the next test was reduced to 55 °C. The mass losses at both temperatures are described in next chapter, in Table 5.

3. Experiment evaluation

3.1. Mass losses evaluation

The values given in Table 5 show that all the investigated alloys were affected by pitting corrosion even at temperatures significantly lower than the theoretical estimate of CPT. However, with increasing PREN, the alloy's mass losses (per area) reached lesser values. Based on the comparison of the specimen of the blade and Alloy 2 (whose mass loss corresponds to a similar PREN value), it can be concluded that the result of the Y block material corresponds to the result of a material from the real part. Therefore, the results for all the Y block specimens can be compared to components with a similar chemical composition in real operation.

Table 5.

Mass loss per unit of surface area compared to PREN and theoretical CPT values

| | | Blade | Al. 1 | Al. 2 | Al. 3 | Al. 4 |
|---|-----------------|--------|--------|--------|--------|--------|
| | PREN | 41,363 | 40.53 | 41.13 | 44.66 | 46.52 |
| | theor. CPT [°C] | 58,417 | 57.997 | 57.886 | 65.937 | 69.878 |
| met. A, Δm/P [g/cm ²] | $21,5 \pm 2$ °C | 0 | 0 | 0 | 0 | 0 |
| | 55 ± 7 °C | 0.1400 | 0.1552 | 0.1516 | 0.1607 | 0.0518 |
| met. E, Δm/P [g/cm ²] | 61 ± 1 °C | 0.0587 | 0.0487 | 0.0561 | - | 0.0393 |
| | 55 ± 1 °C | 0.0541 | 0.0474 | 0.0531 | 0.0484 | 0.0369 |

theor. CPT – theoretical estimation of critical pitting temperature

met. A/E – ASTM G48 – 11 method A/E

Δm/P – Mass loss per unit of surface area

missing data – failure during test

Because Alloys 2 and 3 (which differ mainly in molybdenum content) reached similar mass loss values, it can be stated that the change in the molybdenum concentration did not have such an effect on the pitting corrosion resistance as would be estimated based on the PREN value (or the CPT theoretical estimate).

A significant decrease in weight loss was present only in Alloy 4, which differed from the others mainly by the increased nitrogen content. Minimized manganese content (in Alloy 1) has led to increased corrosion resistance, but the significance of this effect is not sufficient to make it a recommendation-worthy procedure.

3.2. Evaluation of the mechanical properties

The cast Alloys 1 to 4 were subjected to a tensile test and a Charpy impact test. The aim was to determine whether changing the alloy content in favour of increasing the PREN value will affect the mechanical properties. Tensile test specimens were made according to DIN 50125, type B 10x50. Samples for the impact Charpy test (V-notch) were made according to the ČSN EN ISO

148-1 standard, type A 10x55 specimens were used. The values of strength, elongation and toughness are given in **Table 6**. The values from the tensile test ($R_{p0.2}$, R_m , A) given in the table are the average of 2 measured values, the KV values given in the table are the average of 3 measured values. They are compared with the standard values for this steel grade [10].

Table 6.

Average values of the mechanical properties measured

| | Al. 1 | Al. 2 | Al. 3 | Al. 4 | Standard |
|------------------|-------|-------|-------|-------|-----------|
| $R_{p0.2}$ [MPa] | 497 | 498 | 536 | 546 | min. 480 |
| R_m [MPa] | 775 | 786.5 | 817 | 825.5 | 650 – 850 |
| A [%] | 30.55 | 30.35 | 29.8 | 24.1 | 22 |
| KV [J] | 146.1 | 124 | 130.5 | 131.5 | ≥ 50 |

The tests of the mechanical properties show that the change in chemical composition affected the mechanical properties, but all the monitored properties safely met the requirements given by the standard. The measured values show that with an increasing content of the PREN-increasing alloys, the strength increased, while the ductility decreased. This is due to the substitution (in the case of nitrogen interstitial) strengthening of the material. The toughness of Alloy 1 exceeds the others, which reach approximately the same value. All the alloys safely reached the required toughness.

4. Conclusions

- The actual critical pitting temperature (CPT) for 1.4517 steel in cast state is lower than 55 °C, which is significantly lower than the temperature expected due to the chemical composition (57–69 °C in this experiment). The exact determination of the CPT for this steel needs to be achieved through further research.
- A reduction of manganese content (as MnS inclusions act as nucleation sites for localized corrosion) did not lead to increased resistance to pitting corrosion.
- An increase of molybdenum content did not have a significant effect on pitting corrosion resistance in 1.4517 steel, despite its relatively high coefficients in PREN and CPT formulas.
- An increase of nitrogen had a significant positive effect on pitting corrosion resistance (indicated by lesser mass loss), although even its increase above the standard did not lead to measured CPT reaching values estimated by chemical composition.
- Increasing the content of PREN-increasing alloys has led to an increase in strength and a decrease in ductility, but all safely within the ranges specified by the steel grade.

Acknowledgement

The paper was prepared with the support of TAČR within the project ev. no. TH02020076 – “Výzkum a vývoj odlévání a

svařování masivních odlitků z duplexních ocelí” (Research and development of casting and welding of solid duplex steel castings)

References

- [1] Reardon, A. (2011). *12.5 Duplex Stainless Steels. In metallurgy for the non-metallurgist* (2nd Edition). Ohio: ASM International, ISBN 978-1-61503-821-3, Retrieved from <https://app.knovel.com/hotlink/pdf/id:kt009JBTT4/metallurgy-non-metallurgist/duplex-stainless-steels>
- [2] McGuire, M.F. (2008). *Duplex stainless steels. in stainless steels for design engineers* (91–108) [online]. Materials Park, Ohio 44073-000: ASM International, [cit. 2020-05-19]. ISBN 978-1-61503-059-0., Retrieved from: <https://app.knovel.com/hotlink/pdf/id:kt008GRPY2/stainless-steels-design/duplex-stainless-introduction>
- [3] O'Brien, A. ed. (2011) *Stainless and Heat-Resistant Steels. In Welding Handbook, Volume 4 - Materials and Applications, Part 1* [online]. 9th Edition. Miami: American Welding Society (AWS), p. 351 [cit. 2020-05-27]. ISBN 978-1-61344-537-2. Retrieved from <https://app.knovel.com/hotlink/pdf/id:kt0095SGE2/welding-handbook-volume/duplex-sta-composition>
- [4] Revie, R.W. ed. (2011). In *Uhlig's Corrosion Handbook* [online]. Third edition. Duplex stainless steels. (695–705). Hoboken, New Jersey: John Wiley & Sons, 2011 [cit. 2020-06-14]. ISBN 978-1-61344-161-9. Retrieved from <https://app.knovel.com/hotlink/pdf/id:kt008TZY32/uhlig-s-corrosion-handbook/duplex-sta-history>
- [5] Prošek, T. & Šefl, V. (2018). Corrosion resistance of stainless steel in drinking water treatment plants and water storage units. *Koroze a ochrana materialu*. 62(4), 141-147. DOI:10.2478/kom-2018-0020.
- [6] Cicek, V. (2014). *Corrosion engineering*. Hoboken, New Jersey: Scrivener Publishing/Wiley. ISBN 978-1-118-72089-9. Retrieved from <https://app.knovel.com/hotlink/toc/id:kpCE00004B/corrosion-engineering/corrosion-engineering>.
- [7] Marcus, P. ed. (2012). *Corrosion mechanisms in theory and practice*. Third edition. Boca Raton: CRC Press, Corrosion technology (Boca Raton, Fla.). ISBN 978-1-4200-9463-3.
- [8] G48 - 11(2015). Standard test methods for pitting and crevice corrosion resistance of stainless steels and related alloys by use of ferric chloride solution. West Conshohocken: ASTM International, 2015.
- [9] Jargelius-Pettersson, R.F.A. (1998). Application of the pitting resistance equivalent concept to some highly alloyed austenitic stainless steels. *Corrosion*. 54(2), 162-168. DOI:10.5006/1.3284840.
- [10] (2015). Austenitic-ferritic (duplex) casting materials [online]. Otto Junker, 2015 [cit. 2020-06-25]. Retrieved from: <https://www.otto-junker.com/cache/dl-Austenitic-Ferritic-DUPLEX-Casting-Materials-aa4d1dd1db00d37343728c6ba0598a75.pdf>